Synthesis of Nucleoside-Boronic Esters Hydrophobic Pro-drugs: A Possible Route to Improve Hydrophilic Nucleoside Drug Loading into Polymer Nanoparticles

Yasmin Abo-zeid [1, 2], Giuseppe Mantovani[2], Will Irving[3], Martin C Garnett [2]

[1] School of Pharmacy, Helwan University, Cairo, Egypt
[2] School of Pharmacy, University of Nottingham, Nottingham, UK.

Corresponding Author:

Yasmin Abo-zeid

[1]School of Pharmacy, Helwan University, Cairo, Egypt
[2] School of Pharmacy, Boots Building, Science Road, University Park, University of Nottingham, Nottingham, UK, NG7 2RD
E-mail: Yasmin Abozeid@nottingham.ac.uk
Mobile : +44073066025

Co-authors:

Giuseppe Mantovani
[2] School of Pharmacy, Boots Building, Science Road, University Park, University of Nottingham, Nottingham, UK, NG7 2RD
E-mail: giuseppe.mantovani@nottingham.ac.uk

Will Irving,
[3]Faculty of Medicine & Health Sciences, Queens Medical Center, University of Nottingham, Nottingham, UK, NG7 2UH
E-mail: Will.Irving@nottingham.ac.uk

Martin C Garnett
[2] School of Pharmacy, Boots Building, Science Road, University Park, University of Nottingham, Nottingham, UK, NG7 2RD
E-mail: M.Garnett@nottingham.ac.uk

Abstract:

Nucleoside analogues are active therapeutic agents for different types of diseases e.g. Cancer and virus infections. However, they are associated with several side effects due to off-target accumulation. Particulate delivery systems such as nanoparticles (NP) may be able to selectively target drug into affected organs and lower or omit off-target accumulation. Hydrophilic nucleoside analogues are poorly incorporated into NP. This work has used boronic compounds to synthesize more hydrophobic biodegradable pro-drugs of hydrophilic nucleosides to improve drug loading into NP. Ribavirin (RV) was used as a model hydrophilic nucleoside to test our hypothesis. RV is a broad antiviral agent, active against both RNA and DNA viruses. RV accumulates into Red Blood Cells (RBCs) causing haemolytic anaemia that restricts its therapeutic benefits. RBCs are reported to have no endocytic mechanisms. So, NP delivery should be advantageous. Two hydrophobic pro-drugs of RV were synthesized namely, ribavirin conjugated to phenylboronic acid and ribavirin conjugated to 4-butoxy-3, 5-dimethylphenylboronic acid and were encapsulated into polymer NP. It was shown that the pro-drugs were incorporated more effectively into polymer nanoparticles with a 1700 fold improved RV loading. Polymer NP had been prepared with biocompatible and biodegradable polymers, Poly(glycerol adipate) and its more hydrophobic derivatives.

Keywords: Polymer nanoparticles; Poly (glycerol adipate); acylated Poly (glycerol adipate); phenyl boronic acid compounds; hydrophilic nucleoside

1. Introduction:

Nucleoside analogues have been broadly used clinically as anticancer and antiviral agents. Being an antiviral, they have an important role for eradication of life threatening chronic virus infections such as AIDS (1); (2), Hepatitis B (3); (4) and Hepatitis C viruses (HCV) (5); (6) as well as acute virus infection e.g. Influenza virus that could be life threatening for children, pregnant women and elderly people at time of local outbreaks e.g. Spanish Influenza (7). However, nucleosides analogue administration is associated with several side effects that limit its clinical benefit. Zidovudine can induce cardiac and skeletal muscle myopathy (8); (9). Peripheral neuropathy is commonly seen with didanosine and stavudine, lactic acidosis is observed after didanosine, and stavudine administration and can have a fatal outcome due to extreme mitochondrial toxicity (9). Fialuridine, is another nucleoside analogue used for treatment of hepatitis B and it also causes mitochondrial poisoning that has resulted in the death of five patients (10); (11). Application of the following anticancer agents, Fludarabine, Cytarabine, Gemcitabine, Fluorouracil, Capecitabine is mainly associated with myelosuppression as a main side effect (12). A further drawback of nucleoside analogue administration is development of resistance (13) and cross-resistance to other compounds due to up-regulation of the P-glycoprotein drug efflux pump responsible for excretion of toxic compounds and a variety of different drugs (14). Therefore, finding a selective delivery system that could deliver these nucleoside analogues to the target tissue while decreasing or avoid their accumulation in off target tissues and nucleoside resistance due to P-glycoprotein will result in a dramatic improvement of their therapeutic efficacy and safety.

Nanoparticles (NP) are an advanced delivery system and interest in their clinical development for different diseases has been growing over the last couple of decades. Advantages of NP include the ability to control the particle size, modify the particle surface properties and by attaching specific ligands, it could target certain organs or cells. NP have also the ability to sustain drug release. Together, these properties pave the way for more efficient and safe delivery of therapeutic agents. NP involve different particulate systems such as liposomes and polymer nanoparticles, etc. Nanoparticles may be particularly appropriate for liver delivery as the liver filters out nanoparticles very efficiently so there is a prospect for a high localisation of nanoparticles. Whereas for most applications PEGylated polymers are used to enhance circulation of nanoparticles, delivery to the liver may be facilitated by particles which have a low or no PEG surface covering.

Ribavirin (RV) was selected to be used as a model of hydrophilic nucleosides in the current study due to its broad antiviral spectrum against RNA and DNA viruses (15). RV was previously a drug of choice to be used in combination with PEGylated interferon for treatment of HCV (16); (17) and it is still used in some regimen of HCV for patients suffered from Cirrhosis (18); (19) and infected with genotype 1a (20) and genotype 3 (21); (22) and genotype 4 (23) and it has an added value by shorten the duration of treatment for patients with Genotype 1 and compensated Cirrhosis (24). RV in combination with asunaprevir, daclatasvir, vaniprevir plus pegylated interferon alfa 2b have been approved for treatment of Genotype 1 in Japan (25). Furthermore, it is still the recommended drug for HCV treatment in some poor countries due to the high cost of Direct Acting Antivirals (DAA) (26). Although DAA dangerously threaten RV future in HCV treatment, RV is still an antiviral agent that could be used in treatment of chikungunya virus (27); (28), norovirus (29); (30); (31); (32) and it had been used in treatment of outbreaks of dengue virus (33), Hendra and Nipah viruses (34), Marburg

virus (35) and lassa virus (36). Due to the continuous emergence of new viruses and the long time required to develop new and effective antiviral agents. Scientists thought it is beneficial to make use of the currently FDA approved antivirals, especially it is known that viruses from the same family share similar features (37) and therefore might be treated with one of the licensed antiviral agents. Many of the emerging viruses belong to virus's families that are currently being treated with one or more of the licensed antiviral drug (33). Many of licensed antiviral drugs could be used for treatment of viruses belong to different families (38).Therefore, development of a delivery system of the current licensed antiviral agents to improve their efficacy and decrease side effects should have a positive impact on future of antiviral therapy. RV as many other nucleosides analogues, its administration is accompanied by side effect, haemolytic anaemia, due to RV accumulation into Red Blood Cells (RBCs) (39). RBCs are reported to have no endocytic mechanisms (40). Polymer nanoparticles have been extensively investigated for encapsulation of drugs, as they are relatively cheap to produce and a number of different methodologies are available to optimise encapsulation (41); (42); (43). A high level of encapsulation is important to ensure that sufficient drug can be delivered to the target to achieve a useful therapeutic effect. However, a number of publications have reported that hydrophilic molecules e.g. Gemcitabine, Zalacitabin are incorporated to a lower extent than hydrophobic molecules (44); (45). A different strategy is therefore required for encapsulation of these drugs into polymer nanoparticles.

In general, we would expect that a relatively hydrophilic drug would favour partitioning of the drug into the outside aqueous medium, rather than in the hydrophobic core of the NP. Also, it would favour diffusion of the drug from the NP into the surrounding aqueous medium after loading leading to a rapid drug release. In this paper, we hypothesized that synthesis of a more hydrophobic prodrug of hydrophilic nucleoside analogues using boronic acid derivatives might improve nucleoside loading into polymer nanoparticle and hence, its clinical application. However, this hydrophobic pro-drug should be able to degrade under physiological conditions to release the drug (hydrophilic nucleoside) in a therapeutically active form. RV is a purine analogue and so development of a strategy for this drug may also be of relevance for other nucleoside analogues.

We have selected the use of boronic acid derivatives for this strategy due to their distinct properties of selective binding to 1,2 Cis diols which are present in the sugar ring of the nucleoside analogue (46). This should generate a more hydrophobic compound through formation of a reversible boronic ester covalent linkage that can be easily degraded under physiological conditions to yield the active nucleoside analogue. It is worth noting that the end product of boronic ester degradation is boric acid which is reported to have no toxicity to humans (47). In our group we have also developed the poly (glycerol adipate) (PGA) family of polymers. PGA is enzymically synthesised and has a pendant hydroxyl group on every co-monomer unit that can be easily modified with acyl groups to change the hydrophobicity of the polymer which can result in increased drug loading (48).In this paper we have therefore explored the possibility of producing more hydrophobic prodrugs in conjunction with a polymer whose physicochemical properties can be tailored to the drug to enhance the drug loading of nanoparticle formulations.

2. Materials and Methods:

2.1. Materials:

All materials were purchased from Sigma-Aldrich and VWR except divinyladipate purchased from Tokyo Chemical Industry UK Ltd. Phenylboronic Acid Solid Phase Extraction cartridges were purchased from Agilent company. Purified water ELGA, Model ELEC 25 (ELGA 13 KΩ resistivity) while HPLC water (ELGA 18 KΩ resistivity) was used for HPLC work. Ribavirin was granted as a gift by October Pharma Company, Cairo, Egypt.

2.2. Methods:

2.2.1. Synthesis and characterization of PGA and its acylated derivatives:

PGA and its acylated polymers, 20%-C_{18} PGA, 20%-C_8PGA and 40%-C_8PGA were synthesized as previously reported (48), (Figure 1). Briefly, PGA was synthesized by dissolving Equal amounts (250 mmol) of glycerol and DVA in dry tetrahydrofuran (THF, 30 ml) in presence of a catalytic enzyme, Novozyme 435 (1.25 gm) and the reaction was stirred (overhead stirrer, 200 rpm) at constant temp (50˚C) for 24h. This followed by enzyme filtration and evaporation of THF to obtain a yellowish Jelly-like polymer, its Mn, SEC = 11.6 kDa and molecular weight dispersity Đ of 1.4 and the molecular weight (Mw) was around 16 KDa as revealed by SEC characterization.

For Acylated polymers synthesis, Figure 1, the previously synthesized PGA (2.10 g, 10.4 mmol) was dissolved and refluxed (2h) in dry THF (10 ml) in the presence of acyl chloride, either 2.05 mmol or 4.1 mmol and pyridine (2ml) to obtain 20% or 40% acylation percentage respectively. HCl (2M, 100 ml) and Dichloromethane (50 X 3) were used to extract the acylated polymers. Then, organic phase was washed with water (100ml) and dried over magnesium sulfate. The polymer was collected after evaporation of solvent by rotary evaporator. Acylation percentage (20% and 40%) refers to the percentage of hydroxyl groups modified along the polymer backbone.

Gel Permeation Chromatography (GPC) was performed for determination of polymer molecular weight and molecular weight dispersity Đ. Accordingly, polymer samples (20 mg) were dissolved in THF (2 ml) then the solutions were mixed for an hour on the roller-mixer (SRT1, Stuart) to allow the polymers to fully dissolve followed by sample filtration using a syringe membrane nylon filter (0.2 μm) followed by SEC analysis as previously reported (48).

2.2.2. Synthesis and characterization of RV-PBA and RV-BPBA:

Phenyl boronic acid (PBA) and 4-butoxy-3,5-dimethyl phenyl boronic acid (BPBA) were conjugated to ribavirin (RV) using the previous reported methodology (49). Briefly, a pyridine solution of PBA or BPBA (5 mmol in 50 ml of solvent) was added dropwise to equimolar amount of RV dissolved in pyridine (5 mmol, 100 ml) in a 250 ml-RBF. The solution was refluxed for 2 h, then pyridine was evaporated under vacuum. Dry acetone (5 ml) was added into the product and the resulting mixture was then added dropwise into dry diethyl ether (150 ml), the resulting precipitate was filtered off and dried in vacuum desiccator overnight.

2.2.3. ^{1}H-NMR Spectroscopy:

The NMR spectra were recorded on Bruker AVIII HD 400 MHz NMR using a BBFO+ probe and are expressed in parts per million (δ) from internal tetramethylsilane. Polymer samples were dissolved in acetone-d_6. RV-PBA and RV-BPBA, RV, PBA and BPBA were dissolved in acetone-d_6, chloroform-d, DMSO-d_6, acetone- d_6 and chloroform-d respectively.

PGA: ^{1}H NMR (400 MHz, Acetone-d6) δ 5.34 – 5.22 (m, 0H), 5.12 – 5.03 (m, 0H), 4.46 – 3.99 (m, 5H), 3.74 – 3.49 (residual THF), 2.43 – 2.26 (m, 4H), 2.05 (acetone-d6), 1.85 – 1.72 (residual THF),1.70 – 1.58 (m, 4H). **20%C_8PGA:** ^{1}H NMR (400 MHz, Acetone-d6) δ 5.37 – 5.20 (m, 1H), 5.16 – 5.02 (m, 1H), 4.45 – 3.98 (m, 5H), 2.47 – 2.23 (m, 6H), 2.05 (acetone-d6),

1.74 – 1.52 (m, 6H), 1.38 – 1.21 (m, 8H), 0.97 – 0.79 (m, 3H). **40%C_8PGA:** ^{1}H NMR (400 MHz, Acetone-d6) δ 5.38 – 5.20 (m, 1H), 5.12 – 5.02 (m, 1H), 4.42 – 3.94 (m, 5H), 3.74 – 3.49 (residual THF), 2.44 – 2.23 (m, 6H), 2.05 (acetone-d6), 1.85 – 1.72 (residual THF), 1.71 – 1.50 (m, 6H), 1.39 – 1.18 (m, 8H), 0.95 – 0.83 (m, 3H). **20%C_{18}PGA:** ^{1}H NMR (400 MHz, Acetone-d6) δ 5.36 – 5.22 (m, 1H), 5.13 – 5.02 (m, 1H), 4.49 – 3.98 (m, 5H), 2.47 – 2.19 (m, 6H), 2.05 (acetone-d6),1.74 – 1.50 (m, 6H), 1.39 – 1.21 (m, 28H), 0.95 – 0.81 (m, 3H). **RV:** ^{1}H NMR (400 MHz, DMSO-d6) δ 8.87 (s, 1H), 7.86 – 7.79 (m, 1H), 7.61 (s, 1H), 5.81 (d, J = 3.9 Hz, 1H), 5.57 (d, J = 5.6 Hz, 1H), 5.19 (d, J = 5.6 Hz, 1H), 4.91 (t, J = 5.6 Hz, 1H), 4.35 (td, J = 5.2, 4.0 Hz, 1H), 4.13 (q, J = 5.2 Hz, 1H), 3.94 (q, J = 4.8 Hz, 1H), 3.63 (dt, J = 11.9, 5.5, 4.1 Hz, 1H), 3.49 (dt, J = 12.0, 5.3 Hz, 1H). **RV-PBA:** ^{1}H NMR (400 MHz, Acetone-d6) δ 8.76 (s, 1H), 7.82 (dd, 2H), 7.55 (dt, 1H), 7.44 (dt, 3H), 6.40 (d, J = 1.7 Hz, 1H), 5.69 (dd, J = 6.8, 1.7, 0.5 Hz, 1H), 5.39 (dd, J = 6.9, 2.2, 0.6 Hz, 1H), 4.52 (td, 1H), 4.31 (t, J = 5.8 Hz, 1H), 3.83 – 3.73 (m, 1H), 3.71 – 3.63 (m, 1H), 2.05 (acetone-d6). **RV-BPBA:** ^{1}H NMR (400 MHz, Chloroform-d) δ 8.36 (s, 1H), 7.50 (s, 2H), 7.26 (chloroform-d), 6.12 (d, J = 2.0 Hz, 1H), 5.52 (dd, J = 6.9, 2.1 Hz, 1H), 5.34 (dd, J = 6.8, 2.2 Hz, 1H), 3.93 (d, J = 12.6 Hz, 1H), 3.79 (t, J = 6.5 Hz, 3H), 3.22 (s, 2H), 2.5 (DMSO-d_6), 2.30 (s, 6H), 1.88 – 1.72 (m, 2H), 1.54 – 1.47 (m, 1H), 1.00 (t, J = 7.4 Hz, 3H).

2.2.4. Preparation of ribavirin nanoparticles:

2.2.4.1. PGA NP:

The nanoparticle dispersions were prepared by the nano-precipitation method (48). Briefly, PGA (20 mg) was dissolved in acetone (2 ml) to form the organic phase that was added dropwise while stirring into the aqueous phase, ammonium phosphate buffer (1 mM, 5 ml, pH 6.3) containing RV (20 mg). RV-PBA/RV-BPBA PGA NP were prepared in a similar way except that the polymer and RV-PBA or RV-BPBA (10 mg) were dissolved together in acetone or THF respectively (2 ml) and the aqueous phase was HEPES buffer (5 ml, 10 mM, pH 8). The nanoparticle dispersion was left to stir overnight for complete evaporation of organic solvent and formation of NP.

2.2.4.2. Acylated PGA NP:

Acylated polymers were used to prepare NP of the pro-drugs using a nano-precipitation method. The nano-precipitation was carried out as previously described except the organic phase (3ml) and calcium hydroxide (0.3 mM, 5 ml or 10 ml) as an aqueous phase were used instead. A set of 20%-C_{18}PGA NP were also prepared in the presence of Tween 80 (0.05%, relative to the aqueous phase).

2.2.5. Purification of polymer nanoparticles:

All NP were purified to remove un-encapsulated free drug by gel filtration chromatography. The NP sample was loaded onto a sepharose CL-4B column (C2.5 X 40, Pharmacia, bed volume 91ml). The column was eluted using a peristaltic pump at a flow rate of (1 ml/min) and collected in fractions (1.5ml/ tube). Calcium hydroxide (0.5 µM) was used as the eluent for all types of drug loaded NP except RV PGA NP where ammonium phosphate buffer (1 nM, pH 6) was used as an eluent. The peaks of drug containing NP and free drug were detected using a Pharmacia chromatographic UV detector (206nm filter).

2.2.6. Characterisation of nanoparticles:

2.2.6.1. Determination of particle size, size distribution and Zeta potential:

NP dispersion was diluted with HEPES buffer pH 8 either 1 mM or 5 mM for particle size and zeta potential measurements respectively. Samples were diluted to give a count rate of 50 to 300 Kcps and measurements were performed at 25 °C ± 0.1 using Malvern Zeta sizer Nano ZS (Malvern Instruments Ltd, Malvern, UK).

2.2.6.2. Determination of Drug Loading:

RV drug loading had been determined by following the protocol previously reported (50) but with some modifications. A known weight of freeze dried NP was dissolved in an organic solvent [acetone: methanol (1:1), pH 6.5]. The phenylboronic acid cartridges (PBA cartridges) were pre-conditioned with phosphoric acid in methanol (1ml, 0.5% v/v) followed by ammonium phosphate buffer (1 ml x 3, 250 mM, pH ≥ 11.5). After sample (1ml) loading into the pre-conditioned cartridges, the cartridges were eluted with ammonium phosphate buffer (1ml x 3, 250 mM, pH ≥ 11.5), methanol (2ml) and then RV was eluted by addition of formic acid in methanol (1ml x 2, 2.5% v/v). The sample was prepared for HPLC analysis by evaporating the formic acid in methanol using a Juan vacuum centrifuge at 60℃ followed by dissolving the dried extracted RV in purified water (250 µl) and addition of uridine (U) solution (5 µl, 1 mg/ ml, purified water) as an internal standard. The sample was analysed by injection into an HPLC column set consisting of an Atlantis dc18 guard column (4.6 mm X 20 mm, 3 µm) connected to an Atlantis dc18 column (150 mm X 4.6 mm, 3 µm). Ammonium phosphate buffer (10 mM, pH 3.3) was used as a mobile phase at a flow rate of 1ml/min, temperature 40℃ and UV detection at 207nm. The total amount of RV entrapped was calculated from the calibration curve of different known RV concentrations (0.1 to 50 µg/ml) prepared in purified water in presence of U (20 µl, 1 mg/ml, purified water) as an internal standard. Drug loading was calculated as follows,

$$\text{Drug loading Percentage} = \frac{\boldsymbol{Amount\ Drug\ Entrapped\ (mg)}}{\boldsymbol{Weight\ of\ NP(mg)}} * 100$$

To identify the efficiency of RV extraction, equal concentration of RV/ PBA (20, 50 and 100 µg/ml) in the presence of PGA (10 mg) in a mixture of acetone: methanol (1:1) pH 6.5 was extracted with the pre-conditioned phenylboronic acid cartridges as previously described and the amount of the extracted RV samples was reconstituted in purified water (1ml) and U (20 µl, 1mg/ml, purified water) was added followed by sample injection into HPLC. The efficiency of the extraction method was determined via calculation of the recovery percentage as follows;

$$\text{Recovery Percentage} = \frac{peak\ area\ of\ (RV/U)Sample}{peak\ area\ of(RV/U)reference} * 100$$

Peak area of (RV/U) sample; was calculated for the known RV concentrations that had been extracted from the previous RV samples (RV/PBA in presence of PGA) after being treated with pre-conditioned PBA columns followed by HPLC measurement. Peak area of (RV/U) reference; is calculated for samples of similar RV concentrations (20, 50, 100 µg/ml, purified water) in presence of U (20 µl, 1mg/ml, purified water) that had been injected into HPLC directly without any pre-treatment or extraction with PBA columns.

2.2.7. Validation of ribavirin HPLC analysis

HPLC analysis of RV was validated by determining linearity, inter and intra-day variation. RV linearity was determined by using RV concentrations ranging from 0.1 to

50 µg/ml prepared in the purified water. The accuracy and precision of intra- day and inter-day variation were determined using RV concentrations, of 12.5, 25 and 50 µg/ml. Analysis of these concentrations was done three times in the same day at different times (Intra-day variation) and on different days (Inter-day variation). Again uridine (20 µl, 1 mg/ml, purified water) was used as an internal standard. The accuracy and precision were calculated as follows,

$$\text{Accuracy} = [(M-N)/N] * 100$$

M is the mean value of RV concentration measurements while N is the theoretical concentration.

$$\text{Precision (\% RSD)} = [\text{SD/Average}] * 100$$

RSD is the relative standard deviation, SD is the standard deviation of measurements and Average is the mean value of RV concentration measurements.

2.2.8. Investigating the stability of RV-boronic ester linkage

2.2.8.1. In organic phase

RV-PBA or RV-BPBA (10 mg) was dissolved in dry acetone or dry THF respectively (3 ml) and left overnight for complete evaporation of organic solvent. The dried residue was dissolved in DMSO- d_6 (1 ml) and characterised by ^{1}H-NMR.

2.2.8.2. In aqueous phase

RV-PBA/RV-BPBA (10 mg) was added to ammonium phosphate buffers (5 ml, 250 mM, pH 6.5, 7.5, 8, 8.5) or calcium hydroxide solution (5 ml, 0.3 mM) and left to stir for 20h. For RV-PBA, 2 ml of these solutions were freeze dried to remove water. The freeze-dried residue was dissolved in DMSO- d_6 (1 ml) and characterised by ^{1}H-NMR. For RV-BPBA, 1 ml of these solutions was centrifuged and supernatant (0.7 ml) was taken and pH was adjusted into 8.5 using ammonium phosphate buffer (250 mM, pH 8.5). Then, RV was extracted by the pre-conditioned phenylboronic acid cartridges followed by HPLC analysis as described. Ribavirin degradation percentage was calculated by the following equation;

$$Ribavirin\ Degradation\% = \frac{Amount\ of\ ribavirin\ degraded\ (mg)}{Intial\ amount\ of\ ribavirin\ (mg)} * 100$$

Amount of RV degraded represents the amount of RV detected in the supernatant of RV-BPBA samples, Initial amount of RV was determined after dissolving RV-BPBA (10 mg) in acetone: methanol (1:1, pH 6.5) followed by extraction as described in section 2.2.6.2.

2.3. Statistical analysis:

All statistical analysis was done using TWO WAY ANOVA followed by Post-hoc test (Tukey test). Statistical analysis was done by IBM SPSS version 21 at confidence level (95%).

3. Results and Discussion:

3.1. Synthesis and characterization of PGA and its acylated derivatives: A variety of polymers are used to prepare nanoparticles for drug delivery systems, and we believe that PGA has number of advantages over other available polymers. PGA is readily biodegradable with biologically compatible degradation products; adipic acid and

glycerol that are recognized safe compounds as approved by FDA (51) and is unique among biodegradable polymers in being easily chemically modified through the pendant hydroxy group allocated along the polymer backbone to give a range of polymers with different physicochemical properties (48); (52); (53). The green synthesis (enzymatic synthesis) of PGA avoid the harsh conditions (metal catalysts, high temperature required for synthesis around 120°C as well as lack of stero-selectivity) commonly required to prepare other polyester polymers (52). In this work PGA was synthesised by polycondensation of divinyladipate and glycerol in THF at 50 °C for 24 h catalysed by Lipase Enzyme, Novozyme 435 as previously reported (48) and described in Figure 1. PGA synthesis was demonstrated by ^{1}H-NMR through disappearance of DVA vinyl proton peaks at δ 4.5 to 5 ppm and at δ 7.5 ppm in addition to appearance of broad polymer signals – *e.g.* methylene groups peaks of the adipate repeating units at δ 1.6 and 2.37 ppm (Figure S1, Supplementary Information). The resulting PGA possessed mostly linear macromolecular architecture, with largely predominant (85%) 1,3-diesterified glycerol repeating units. 1,2-diester units (7.5% mol/mol) were also observed by ^{1}H NMR along with 1,2,3-tri-ester branching residues (7.5%) (Figure S2, Supplementary Information) resulting in an overalls side branching that does not exceed 15%. The latter had been performed by comparing the integration of methine group at δ 5.1 and 5.3 ppm respectively to the peak integration of methylene group either at δ 1.65 or 2.37 ppm as previously reported (54). However, this might be slightly underestimated side branching figure due to incomplete removal of THF. SEC analysis using THF as the mobile phase gave an estimated $Mn_{n,SEC}$ = 11.6 KDa and molecular weight dispersity Đ of 1.4 and molecular weight (Mw) = 16 KDa. Subsequent partial esterification of the PGA residual hydroxyl functionalities with octanoic (C_8) or octadecanoic (C_{18}) acid chlorides was carried out to obtain the acylated 20%-C_8PGA, 40%-C_8PGA, and 20%-C_{18}PGA polymer derivatives (Figure 1). Acylation reaction was demonstrated by appearance of methyl group at δ 0.9 and methylene group at δ 1.3 ppm (Figure 2). The degree of acylation was determined by ^{1}H.NMR spectroscopy (Figures S3:S5, Supplementary Information). The acylation of PGA polymer is resulting in an increase of the 1,2,3-tri-ester branching residues and therefore, the integration of methine CH group (C2) at δ 5.3 ppm will be increased. Therefore, the relative increase of methine group integration was used to calculate the acylation reaction efficiency as follows;

$$\boldsymbol{The\ acylation\ Reaction\ Efficiency} = \frac{[(\boldsymbol{Peak\ C2\ integration\ (acylated\ polymer)} - \boldsymbol{Peak\ C2\ integration\ (PGA)}]}{[\boldsymbol{Peak\ C2\ integration\ (acylated\ PGA)}]} * 100$$

The acylation reaction was more efficient for octanoic (C_8) acid chloride than the octadecanoic (C_{18}) acid chlorides resulting in acylation percentage of 15%, 33.6% and 11% for 20%C_8PGA, 40%C_8PGA and 20%C_{18}PGA respectively. The acylation reaction of PGA was associated with an increase in the molecular weight (Mw) of polymers, as observed by SEC and it was 161000, 91000, and 105,000 Da for 20%C_8PGA, 40%C_8PGA and 20%C_{18} PGA respectively. However, it reflects the size of the polymer rather than an accurate value of the polymer molecular weight. This is mainly due to calibration of SEC with polystyrene, a linear polymer (without pendant groups) and therefore the results obtained for the acylated polymers (20%C_8PGA, 40%C_8PGA, etc) could not be directly correlated to their molecular weight and therefore are not considered as a relevant molecular weight. However, the values recorded for acylated polymers are higher than that recorded for PGA (linear polymer without pendant groups). This could be indicative for the success of acylation reaction of polymer.

3.2. Synthesis and characterisation of RV-PBA and RV-BPBA:

Ribavirin boronic derivatives were synthesized (Figure 3) as previously reported (49) to increase the hydrophobicity of RV and hence its ability to be incorporated within hydrophobic polymeric carriers. Chemical modification was carried out by conjugation of hydrophobic moieties to RV, through formation of a biodegradable boronic ester linkage. The synthesis reaction was carried out in a 250 ml-RBF using an equimolar amount of RV and phenyl boronic acid (PBA) or 4-butoxy-3,5-dimethylphenylboronic acid (BPBA), and following extraction and purification, afforded the desired ribavirin boronic esters in 77% and 69% yields for RV-PBA and RV-BPBA, respectively. Virtually complete conversion of ribavirin into RV-PBA and RV-BPBA was confirmed by ^{1}H NMR analysis (Figure 4) which showed the appearance of HCOB peaks 4 and 3 at δ 5.4 and 5.65 ppm respectively, along with that of phenyl proton peaks at δ 6.5 - 7.9 ppm.

3.3. Drug Extraction from nanoparticles and validation of HPLC analysis

For development and validation of an extraction method for drug quantitation from nanoparticles loaded with RV-boronic acid derivatives, samples simulating the RV-boronic acid derivatives loaded into nanoparticles were prepared. Each sample contained a known weight of PGA polymer and appropriate amounts of RV and PBA at equal concentration. Drug was extracted from these samples to determine the efficiency of the extraction methodology.

The extraction method was based on the protocol that was reported by Arianna with some modifications (55). The principle of the extraction method depends on the lability of the boronic ester linkage at acidic pH. The boronic ester linkage is formed and has a high stability at alkaline pH while it degrades at acidic pH. To extract RV from polymeric NP, an acidic organic solvent (acetone: methanol (1:1), pH ≤ 6.5) was used to dissolve the polymeric matrix and cleave the boronic ester linkage releasing RV. RV was then extracted with pre-conditioned PBA cartridges. Pre-conditioned PBA cartridges should offer an alkaline pH-dependant specific and selective interaction between Cis-diol group of ribose moiety of RV and boronate groups of PBA cartridges to form boronic ester link and therefore RV becomes selectively attached to PBA cartridges. To elute RV for HPLC analysis, an acidic solvent (formic acid in methanol, 2.5%) was used to break down the boronic ester linkage. HPLC analysis showed that RV and U peak retention times appeared at 5.2 and 8.8 minutes respectively (Figure S6, Supplementary Information). The extraction efficiency was expressed as the recovery percentage ± (%RSD), and it was found to be 91% ± 5.2 (RSD%), 97 ± 2 and 100% ± 3.6(RSD%) for 20, 50 and 100 µg/ml respectively. Validation of HPLC analysis method showed that a calibration curve for RV concentrations ranging from 0.1 to 50 µg/ml was linear with a correlation coefficient (R^2) equal to 0.999. Limit of Detection (LOD) and Limit of Quantification (LOQ) were equal to 0.616 and 1.86 µg/ml respectively. Three different concentrations of RV (12.5, 25, 50 µg/ml) were used to evaluate intra-day and inter-day variations using U (20 µl, 1 mg/ml, purified water) as an internal standard. The accuracy of intra-day and inter-day variation ranged from 0.14 to 0.78 and from 1.8 to 3 respectively. The precision (Practical %RSD) ranged from 0.04% to 0.45% for intra-day variation and from 1.06% to 2.4% for inter-day variation indicating a high degree of repeatability. In accordance with AOAC guidelines (56; 57), the following equations were used to calculate the theoretical RSD% for intra-day and inter-day variation respectively, % RSD of repeatability = $C^{-0.15}$ and % RSD of repeatability = $2\ C^{-0.15}$ where C is the analyte concentration expressed as mass fraction. The accepted

practical %RSD for a valid method should range between ½ and 2 times of the theoretical calculated values. Those values that were obtained in the present study indicating the validity of the method used for RV analysis.

3.4. Characterisation of nanoparticles and drug loading

3.4.1. Particle size and Zeta potential measurements:

The particle size measurements of RV, RV-PBA, and RV-BPBA nanoparticles prepared with PGA, 20%-C_8PGA and 40%-C_8PGA, 20%-C_{18}PGA were performed in HEPES buffer (1mM, pH 8) to prevent breakdown of encapsulated boronic acid derivatives. Nanoparticle samples were prepared in triplicate and particle size for all nanoparticles are presented as the average value of particle size diameter (nm). The particle size of RV/RV-PBA/ RV-BPBA NP prepared with PGA polymer was 85, 99, and 88 respectively and their sizes were non-significantly ($P > 0.05$) different from the particle size of the BLANK PGA nanoparticles 104, Table 1.

Use of acylated polymers to prepare RV-PBA/RV-BPBA NP in absence of Tween 80 produces significantly ($P < 0.05$) larger particle size (about 129 to 190 nm) than NP prepared with PGA polymer. NP prepared with 20% and 40% C_8PGA polymers had a particle size range, 140-160nm although the particles with a significant drug loading were slightly larger, about 170nm. NP prepared with 20%-C_{18} PGA polymer have a similar size to NP prepared with C_8PGA polymers except RV-BPBA C_{18}PGA NP (drug conc,1mg/ml) had a larger particle size, 190nm. Another set of C_{18}PGA NP was prepared in presence of Tween 80 and it resulted in a significant ($P < 0.05$) decrease of particle size for RV-PBA NP to be around 100nm while the size of RV-BPBA NP was either the same (190nm) or larger (269nm).

The poly dispersity index (PDI) for nanoparticles prepared with PGA, 20%-C_8PGA and 40%-C_8PGA was small indicating high degree of homogeneity and a low tendency of particle aggregation. In contrast, the PDI of NP prepared with 20%-C_{18}PGA was much higher than those prepared with C_8PGA polymers and this is indicative of a high tendency to aggregate formation. Consequently, 0.05% Tween 80 was added during the nanoprecipitation to control the aggregate formation. However, Tween 80 had a little effect on the polydispersity of RV-PBA NP, while for the BPBA derivative, the polydispersity remained the same and particle size was the same or larger and this indicated the little effect of tween to control particle aggregation.

The larger particle size obtained for acylated polymers compared to PGA polymer may be due to the size of the acyl groups that might increase the size of the particle core or alternatively by an increase in the aggregation number due to the increase hydrophobicity of the polymer (48). Bilati and his colleagues (58) reported that organic solvent with a lower dielectric constant resulted in nanoparticles with a larger particle size. Guhagarkar and his colleagues (59) reported a decrease of the particle size when Acetone: THF (1:1) were used as a solvent compared to the particle size obtained using THF alone as a solvent and it was rationalized to the rapid diffusion of the more polar solvent resulting in rapid precipitation of the polymer that favours formation of small particles. Therefore, solvent may have an effect on the particle size produced from different polymers.

Surfactant addition may enhance NP formation due to (1) reduction of the surface tension of the polymer during particle formation when the latter came into contact with water and so promote the polymer assembly into NP (2) The possibility of interaction

of the acyl chain of surfactant with the polymer may enhance the packing of polymer molecules and hence, a small particle size could be obtained (48). Tween 80 is a non-ionic surfactant that could stabilize NP through steric effects. As a simple nanoparticle surface interaction, this might reduce the tendency of nanoparticles to aggregate which may result in smaller nanoparticles where it is expected that Tween will form a monolayer coat around nanoparticles. It had been reported (60) that 10 µg of Tween 80/Unit mg of NP is required to form a monolayer coat around PLGA NP (no drug was included), have a size 150nm at Tween80 concentration 0.05%. It had been found that there are no significance changes of the amount of Tween80 adsorbed onto the surface of NP or NP size upon increasing the concentration of Tween80 and this is indicative of surface saturation. This is matched with the previous reported data (61) where adsorption of Tween 80 onto the surface octadecyltriethoxysilane resulting in formation of a monolayer of 2nm thickness. Nanoparticles prepared with 20%-C_{18}PGA polymer have a size ranged from 129 to 190nm and therefore, it was expected that Tween 80 (0.05%) should be enough to stabilize the system but there may be a range of much more complex interactions as the nanoparticles form that could involve the drug and surfactant as well as the polymer and surfactant. The surfactant could interact in ways which affect the aggregation number of polymer and drug molecules resulting in either smaller or larger particles depending on whether a smaller or larger number of interactions were favoured. This may be influenced by the hydrophobicity or other properties of the drug present. Diclophenac chitosan nanoparticles (62) prepared in presence of different concentration of Tween 80; 0%, 0.01%,0.02% and 0.03% have a particle size 108nm, 110nm, 128nm and 148nm respectively. Upon tracking the precipitation rate of formulations prepared at 0.03% and 0.02% of Tween 80, it was found that nanoparticles precipitated out from the solution after 24h and 48h respectively. It was expected that an increase of surfactant concentration should keep the stability of the formulation, but it wasn't the case. In the current study Tween 80 had imparted an initial decrease of the particle size of RV-PBA 20%-C_{18}PGA NP while no change or an increase of the particle size for RV-BPBA C_{18}PGA NP but all nanoparticles prepared with 20%-C_{18}PGA polymer had a high PDI value $\geq$ 0.3 and this is indicative of the instability of the system with tendency of particle aggregation. Another study that had been performed by Navneet and his colleagues where Tween 80 was used as a co-surfactant at concentration 0.05%, had resulted in decreasing the particle size of paclitaxel nanoparticles prepared with PLGA from 438 to 389nm but it was accompanied by an increase of PDI from 0.19 to 0.39 and this is indicative of system instability with a high tendency of particle aggregation (63). Tween 80 was added in the present work in a small quantity to minimize possible downstream problems, as it was reported that polysorbate addition could alter the in vivo particle bio-distribution at high surfactant concentration (64).

The zeta potential data of all NP were presented as Zeta potential (mv) ± SD where all sample measurements were performed in HEPES buffer (5mM, pH 8). All NP were stable as indicated by the high negative zeta potential value, around -50 mV, Table 1. The negative surface charge is attributed to the free COOH group in each polymer chain that could result in charge stabilisation and therefore a lower possibility of aggregate formation. The closeness of zeta potential value for NP prepared with different polymers might be due to the choice of HEPES buffer (5mM, pH8) for the zeta potential measurements. The alkaline pH is essential for the stability of the boronic ester linkage of pro-drugs but it also ionizes all carboxylic group presents on the polymer chain. It was expected that addition of Tween 80 might reduce the negative value of zeta

potential due to polyethylene-oxide groups of Tween 80 (48) but this was not seen in the current study. This may be due to the short chain length of PEG in Tween, and the low concentration of Tween 80 used which may result in a low particle surface coverage of surfactant and consequently a flattened PEG layer which was too thin to influence the zeta potential.

3.4.2. Drug loading

In many drug encapsulation studies there is a relatively inefficient separation of free drug from encapsulated drug resulting in quite high drug loadings with rapid apparent drug release. We have used a gel filtration separation resulting in a very efficient removal of all free drug to give a more accurate measure of drug loading.

To determine drug loading, drug was efficiently extracted from the NP using pre-conditioned PBA cartridges as previously described in section 2.2.6.2. RV is a hydrophilic drug and it is expected to have a very low drug loading into polymer nanoparticles and therefore polymers of different physicochemical properties, PGA and acylated PGA were used to prepare NP of RV-boronic derivatives of different hydrophobicity to investigate conditions that may improve drug loading. Due to problems with NP aggregation during NP preparation with acylated polymers, calcium hydroxide solution (0.3 mM) was used as the aqueous medium instead of HEPES buffer (10 mM, pH 8). This aqueous phase offered the alkaline pH necessary for the stability of boronic ester linkage and had a minimum polymer aggregation with a good yield of NP formation.

PGA NP: RV NP prepared with PGA polymer showed a very low % drug loading. 0.001 ± 0.001. This figure is much lower than other reported results for drug loading of nucleosides into biodegradable polymer nanoparticles and may result from the very efficient separation method used in the present work. The drug loading for RV-PBA and RV-BPBA was 0.002 ± 0.001 and 0.001 ± 0.000 respectively, Table 1. So, the use of RV pro-drugs with PGA polymer did not improve drug loading. Acylated PGA polymers were therefore also investigated in these drug loading studies.

Acylated PGA NP: PGA was functionalized with different acyl chain length (C_8/C_{18}) and different acylation percentage (20% and 40%) to produce polymers with different hydrophobicity and were used to prepare nanoparticles of RV boronic derivatives.

At a pro-drug concentration of 1mg/ml, 20%-C_8PGA polymer had a slight enhancement of RV-PBA drug loading (0.025 ± 0.020), however, other combinations of C_8PGA polymers with RV-PBA showed no improvement of drug loading over that achieved by RV PGA NP. In contrast, there was a marked improvement of drug loading for Nanoparticles of RV-BPBA, where 40%-C_8PGA and 20%-C_8PGA polymers, at a pro-drug concentration of 2 mg/ml had 700 times (0.7 ± 0.4) and 1700 times (1.7 ± 1) increase of drug loading respectively, Table 1.

Using 20%-C_{18}PGA polymer in absence of tween 80, only RV-BPBA at a prodrug concentration 2mg/ml (0.056 ± 0.050) showed an improvement of drug loading over RV PGA NP. In the presence of tween 80, a doubling of drug loading (0.134 ± 0.050) for RV-BPBA at the same drug concentration was recorded. While at RV-BPBA concentrations; 1 mg/ml drug loading (0.100 ± 0.100) was improved by 100 times, Table 1. Drug loading of RV boronic derivatives achieved by Nanoparticles prepared with

Table 1: Physicochemical characteristics and drug loading of RV, RV-PBA and RV-BPBA nanoparticles prepared with PGA, 20%-C_8PGA, 40%-C_8PGA and 20%-C_{18}PGA polymers

Sample Name (Drug Conc, mg/ml)	***P. S. dnm [SD] (PDI)**	***Zeta Potential ± SD**	***% Drug Loading ± SD**
BLANK PGA (0)	104 [13] (0.1)	-56 ± 13	-------
RV PGA (4)	85 [11] (0.13)	- 47 ± 12	0.001± 0.001
RV-PBA PGA (2)	99 [8] (0.14)	- 67.9± 13	0.002 ± 0.001
RV-BPBA PGA (2)	88[10] (0.14)	- 50 ± 15	0.001 ± 0.000
RV-PBA 20% - C_8 PGA (1)	152 [2] (0.05)	- 69 ± 8	0.025 ± 0.020
RV-PBA 20% - C_8 PGA (2)	167 [8] (0.09)	- 65 ± 11	0.001± 0.000
RV-PBA 40% - C_8 PGA (1)	148 [1] (0.1)	- 64 ±10	0.001 ± 0.000
RV-PBA 40% - C_8 PGA (2)	138 [5] (0.07)	- 63 ±10	0.001 ± 0.000
RV-BPBA 20% - C_8 PGA (1)	143 [7] (0.16)	- 41± 9	0.150 ± 0.130
RV-BPBA 20% - C_8 PGA (2)	175 [5] (0.12)	- 44 ± 9	1.700 ±1.000
RV-BPBA 40% - C_8 PGA (1)	138 [9] (0.25)	- 52 ±10	0.050 ± 0.030
RV-BPBA 40% - C_8 PGA (2)	170 [14] (0.13)	- 51 ±10	0.700 ± 0.400
RV-PBA 20%- C_{18}PGA (1)	156 [3] (0.5)	- 33 ± 13	0.003 ± 0.001
RV-PBA 20%- C_{18}PGA (2)	136 [6] (0.4)	- 52 ±16	0.004 ± 0.003
RV-BPBA 20%- C_{18}PGA (1)	190 [42] (0.4)	- 59 ±12	0.004 ± 0.003
RV-BPBA 20%- C_{18}PGA (2)	129 [22] (0.4)	- 55 ±23	0.056 ± 0.050
RV-PBA 20%- C_{18}PGA (1) plus Tween 80	106[17] (0.4)	- 47±12	0.004 ± 0.003
RV-PBA 20%- C_{18}PGA (2) plus Tween 80	107 [0] (0.3)	- 54 ±15	0.010 ± 0.010
RV-BPBA 20%- C_{18}PGA (1) plus Tween 80	193 [36] (0.4)	- 54 ±15	0.100 ± 0.100
RV-BPBA 20%- C_{18}PGA (2) plus Tween 80	269 [110] (0.3)	- 56 ±13	0.134 ± 0.050

*Average of 3 samples – Drug Conc; Drug Concentration (mg/ml), P.S; Particle size (diameter, nm), SD; Standard Deviation, PDI; polydispersity index,

20%-C_{18}PGA polymer showed a slight improvement over that achieved by PGA polymer but still significantly ($P < 0.05$) very low compared to drug loading achieved

by C_8PGA polymers. This is probably due to the high tendency of 20%-C_{18}PGA polymer to form aggregates, as a result of their long acyl chain length and very high hydrophobicity. Overall, the presence of tween was not very successful in controlling aggregation but did lead to some increase in drug loading. RV-boronic derivatives have more hydrophobic properties; RV-BPBA> RV-PBA> RV, Table 2. Although, it was believed that both RV-boronic derivatives should be accompanied with an improvement of drug loading, this was only found with RV-BPBA. Also, it was expected that increasing hydrophobicity of polymers (increased acyl substitution, increased acyl chain length) would be associated with an increase of drug loading. However, the highest drug loading was achieved with 20%-C_8PGA polymer which has intermediate hydrophobicity. This led us to two questions, (1) why RV-PBA did not achieve any marked improvement of the drug loading? - and (2) what is the relationship between hydrophobicity and drug loading?

The first question led us to a further investigation about the stability of both RV-boronic derivatives under the conditions of nanoparticle preparation. The stability of RV-PBA and RV-BPBA was investigated in both organic and aqueous phases.^{1}H.NMR analysis was used to estimate the degradation percentage of boronic ester linkage in organic phase and RV-PBA stability in aqueous phase while HPLC analysis was used to track degradation of RV-BPBA in the aqueous phase. RV-BPBA and RV-PBA degradation percentage in organic phase was calculated from ^{1}H.NMR spectra and it was found to be 39% (Figure 5) and 45% (Figure 6) respectively. HPLC analysis showed that RV-BPBA degradation percentage in ammonium phosphate buffers ranged from 27.6% to 33% and the least degradation was in calcium hydroxide solution, 23%. In contrast, RV-PBA was almost completely degraded in all aqueous media (Figure 7). Therefore, the higher stability of RV-BPBA under the conditions of NP preparation could account for the higher drug loading achieved for RV–BPBA and the lack of drug incorporation by RV-PBA. The sensitivity of these drugs to degradation may also have been responsible for the variability seen in some of the drug loading results for RV-BPBA. The remaining amount of stable pro-drugs in the solution under the condition of nanoparticle preparation should be available to be incorporated into the polymer nanoparticles. Therefore, the drug loading percentage determined for each pro-drug/polymer formulation could reflect the stability of the pro-drug loaded into nanoparticle. The full degradation of RV-PBA prodrug means that RV rather than RV-PBA will be available to be incorporated into the polymer nanoparticle and therefore, no marked improvement of drug loading percentage had been recorded, see Table 1. For RV-BPBA, 40% of initial intact pro-drug is still stable under the condition of nanoparticle preparation and is available for incorporation into polymer nanoparticles. Therefore, it was associated with an improvement of drug loading percentage. However, the improvement of drug loading differs for each polymer used for nanoparticles preparation.

RV-BPBA achieved the highest drug loading in the following order for these polymers 20%-C_8PGA > 40%-C_8PGA > 20%-C_{18}PGA, this indicate that drug loading is not directly related to the hydrophobicity for this particular drug, so is there some other relationship between hydrophobicity and drug loading?

The hydrophobicity of a compound is expressed by its Clog P value. The values presented in Table 2 is Clog p values for a single basic unit of PGA polymer (co-monomer of glycerol and divinyl-adipate), its acylated derivatives, the methyl ester of C_8 and C_{18} moieties, RV and RV-boronic derivatives. These Clog P values have been calculated using Chemdraw software. Moving from a negative to a positive value of Clog P is indicative of a change from a hydrophilic to a hydrophobic compound with greater values indicating an increase of the hydrophobic properties of the compound.

Table2: Clog P value for Polymers, acyl methyl esters, RV and RV boronic derivatives

Polymer	*Clog P	Acyl methyl ester	*Clog P	Drug/Pro-drug	*Clog P
PGA	-0.38				
C_8PGA	4.17	C_8 methyl ester	3.36	RV	-2.85
C_{12}PGA	6.29	C_{12} Methyl ester	5.47	RV-BPA	-1.14
C_{18}PGA	9.46	C_{18} Methyl ester	9.62	RV-BPBA	1.36

*Clog P value, a parameter measures the hydrophobicity of the compound. Clog P values were calculated using Chem-draw software. Negative charge indicates increasing hydrophilicity. Clog P value for PGA represents its basic unit and this means that the Clog P value for the polymer backbone should be higher depending on the polymer molecular weight.

Therefore, polymers could be arranged according to an increase of the hydrophobic properties as follows PGA< C_8PGA<C_{12}PGA< C_{18}PGA. This aligned with the increase of the hydrophobicity of the methyl ester of the acylated chains; C_8 methyl ester < C_{12} methylester < C_{18} methylester. It is worth noting that Clog P value presented in the table represented 100% acylation of the single basic unit of PGA while in the current study, polymer acylation had been performed using two different percentage; 20% and 40% using the acyl chloride of C_8 and C_{18}. Although it was not possible to get sensible calculations from Chemdraw for these more complex mixtures of monomers, the more acylation percentage, the higher hydrophobic properties of the polymer and consequently a higher Clog P value is expected. Values for C_{12} PGA and C_{12} methylester was calculated and presented to show the direct proportionality between the increase of acyl chain length and the increase of Clog P value. The hydrophobicity of compounds was a concern because it is believed that the hydrophobicity might have a role in drug loading and this could be through hydrophobic attraction forces (e.g. van der waals attraction forces) between the aromatic rings of the boronic compounds derivatives and the acyl chains of acylated polymers in the aqueous phase and therefore an improvement of drug loading. Furthermore, the hydrophobicity of the compounds/polymers might have an effect on the precipitation rate of compounds/polymers in the aqueous phase. We believe that the co-precipitation of compound and polymer might be accompanied by enhancement of drug loading into polymer nanoparticles.

Bodmeier and McGinity (65) reported that the successful entrapment of drug within the nanoparticles depends on several factors; (a) low solubility of drug in the aqueous phase; (b) a fast rate of precipitation/solidification of the polymer in the organic phase which in turn depends on high aqueous phase solubility and high vapor pressure of solvent, and low viscosity of the internal phase; and (c) high solid-state solubility of

drug in the polymer and this is indicative of high compatibility and miscibility between drug and polymer.

For Nanoprecipitation method, the organic solvent should be miscible with the aqueous phase and have a high vapour pressure (high evaporation rate), this allows rapid precipitation of the polymer with a lower tendency of the drug to escape into the aqueous medium. RV-BPBA is a hydrophobic compound and consequently it preferentially partitions into the organic phase and only escape slowly into the aqueous phase. Therefore, rapid evaporation of organic solvent is accompanied by precipitation of the drug and the polymer. At this stage, another factor will play an important role in drug loading and it is the rate of precipitation of both polymer and drug. We believe, if they have a similar or close rate of precipitation, this will result in a high drug loading but if the rate of precipitation differs, this will be accompanied by a low drug loading. The hydrophobicity of the compound/polymer will likely control the rate of precipitation. Clog P value of C_8PGA is much closer to RV-BPBA than C_{18}PGA polymer (table 2) and therefore we expect (1) a high hydrophobicity of C_{18}PGA compared to RV-BPBA, may result in aggregation of that component separately and so becoming unavailable for co-incorporation into nanoparticles (2) a more similar precipitation rate for C_8PGA and RV-BPBA with a high opportunity for co-precipitation forming nanoparticles (3) a better miscibility and compatibility between RV-BPBA/C_8PGA than RV-BPBA/C_{18}PGA. This could be mediated either through better physical interaction and/or possibly less phase separation of the pro-drug from the polymeric matrix (66). All together, these processes allow a better chance for RV-BPBA to be entrapped into C_8PGA and consequently a higher drug loading for C_8PGA than C_{18}PGA. This could also explain the slightly higher drug loading achieved for RV-BPBA with 20%C_8PGA (1.7 ± 1) versus 40%C_8PGA (0.7 ± 0.4). The Organic solvent may also influence drug loading, Guharkarkar et al (59) reported that Acetone: THF (1:1) resulted in a lower drug loading compared to THF and this was rationalized to the rapid diffusion of the acetone that might be associated with a high tendency of the drug to escape to the aqueous phase. The poor stability of these pro-drugs in aqueous solvent may help to accentuate any differences of hydrophobicity and may partly explain the high variability seen in the drug loading results.

Ishihara and his colleagues (67) reported a drug loading of (1.6 ± 0.2) for ribavirin monophosphate loaded into polylactic acid (PLA) together with an arabanogalactan-polylysine copolymer in the presence of iron. The loading of RMP depended on the ionic bridge between the phosphate group of RMP and the carboxy group of PLA with the iron (III) ion to enhance drug loading of ribavirin. It is noteworthy that we have achieved a similar drug loading, through consideration of hydrophobic interactions between drug and polymer.

4.Conclusion:

Nucleoside analogues are the leading therapeutic agents for treatment of many critical diseases such as Cancer, AIDS, hepatitis B and C. Their therapeutic benefit is compromised due to side effects accompanying their clinical administration. Nanoparticles as an advanced delivery system could encapsulate and target nucleoside analogues to the diseased organ and minimize or prevent their side effects. However, low drug loading of the hydrophilic nucleoside analogues into nanoparticles remains an obstacle. This article reports a new idea that could selectively convert a hydrophilic nucleoside with a vicinal diol into a more hydrophobic biodegradable pro-drug through

formation of the boronic ester linkage to improve the drug loading. RV drug loading was improved enormously (average 1700 times) by developing the more hydrophobic boronic ester pro-drugs (RV –BPBA) and this massive increase of drug loading appeared to depend on the polymer and pro-drug having similar hydrophobic properties. These studies showed however, that sufficient encapsulation was also dependent on the stability of the pro-drug, so further improvements may be seen by the selection of boronic acid reagents which result in more stable boronic acid esters. This may also require a further optimisation of polymer through acyl or other modifications e.g. boronic compounds to obtain the best combination of polymer and drug properties for this novel route of nanoparticle development.

5- Declaration of Interest

The authors declare no conflicts of interest

Acknowledgment: This work had been supported by the Egyptian Culture Centre and Educational Bureau. Ribavirin was granted as a gift by October Pharma Company – Cairo – Egypt.

6- References

1. *Nucleoside reverse transcriptase inhibitor-reducing strategies in HIV treatment: assessing the evidence.* **Orkin, C., et al.** 2018, HIV Medicine , Vol. 19, pp. 18-32.

2. *The development of antiretroviral therapy and its impact on the HIV-1/AIDS pandemic.* **Samuel, Broder.** 2010, Antiviral Research , Vol. 85, pp. 1-18.

3. *Nucleoside Analogues for Chronic Hepatitis B:Antiviral Efficacy and Viral Resistance.* **George, V. Papatheodoridis, Evangelini, Dimou and Vasilios, Papadimitropoulos.** 7, 2002, The American Journal of Gastroenterology, Vol. 97, pp. 1618-1628.

4. *Adherence to Nucleoside/Nucleotide Analogue Treatment in Patients with Chronic Hepatitis B.* **Emin, Ediz Tütüncü, et al.** 2017, Balkan Med J , Vol. 34, pp. 540-545.

5. *Development of antiviral drugs for the treatment of hepatitis C at an accelerating pace.* **De Clercq, E.** 2015, Rev Med Virol , Vol. 25, pp. 254 - 267.

6. *De Clercq E. 2014. Current race in the development of DAAs (directacting actingantivirals) against HCV.* **De Clercq, E.** 2014, Biochem Pharmacol , Vol. 89, pp. 441-452.

7. *Updating the accounts: global mortality of the 1918 - 1920 Spanish influenza pandemic.* **Johnson, NP and Mueller, J.** 76, 2002, Bull Hist Med, pp. 105 - 115.

8. *Mitochondrial dysfunction and nucleoside reverse transcriptase inhibitor therapy: experimental clarifications and persistent clinical questions.* **Lewis, W.** 2003, AntiViral Research, Vol. 58, pp. 189-197.

9. *Clinical manifestations and management of antiretroviral nucleoside analog-related mitochondrial toxicity, Clinical Therapeutics.* **Moyle, G.** 2000, Clin. Ther., Vol. 22, pp. 911-936.

10. *Hepatic Failure and Lactic Acidosis Due to Fialuridine (FIAU), an Investigational Nucleoside Analogue for Chronic Hepatitis B.* **McKenzie, R., et al.** 1995, N. Engl. J. Med., Vol. 333, pp. 1099-1105.

11. *Mechanisms for the anti-hepatitis B virus activity and mitochondrial toxicity of fialuridine (FIAU).* **Colacino, J. M.** 1996, AntiViral Research, Vol. 29, pp. 125-139.

12. *Nucleoside analogues and nucleobases in cancer treatment.* **Carlos, M. Galmarini, John, R. Mackey and and Charles, Dumontet.** 2002, THE LANCET Oncology, Vol. 3, pp. 415- 424.

13. *Nucleoside analogues: mechanisms of drug resistance and reversal strategies.* **Galmarini, CM., Mackey, JR. and Dumontet, C.** 2001, Leukemia, Vol. 15, pp. 875–890.

14. *Low level of mitochondrial deoxyguanosine kinase is the dominant factor in acquired resistance to 9-beta-D-arabinofuranosylguanine cytotoxicity.* **Lotfi, K., et al.** 2002, Biochem Biophys Res Commun, Vol. 293, pp. 1489-1496.

15. *Broad-spectrum antiviral activity of Virazole: 1-beta-Dribofuranosyl-D-Broad-spectrum antiviral activity of Virazole: 1-beta-Dribofuranosyl-.* **Sidwell, RW., et al.** 1972, Science, Vol. 177, pp. 705–706.

16. *Peginterferon alfa-2a plus ribavirin for chronic hepatitis C virus infection.* **Fried, MW., et al.** 2002, N Engl J Med, Vol. 347, pp. 975–982.

17. *Peginterferon alfa-2a plus ribavirin for chronic hepatitis C virus infection in HIV-infected patients.* **Torriani, FJ., et al.** 2004, N Engl JMed, Vol. 351, pp. 438–450.

18. *Efficacy of Sofosbuvir Plus Ribavirin With or Without Peginterferon-Alfa in Patients With Hepatitis C Virus Genotype 3 Infection and Treatment-Experienced Patients With Cirrhosis and Hepatitis C Virus Genotype 2 Infection.* **Foster, GR., et al.** 2015, Gastroenterology, Vol. 149, pp. 1462-1470.

19. *Retreatment of HCV with ABT-450/r-ombitasvir and dasabuvir with ribavirin.* **Zeuzem, S., et al.** 2014, N Engl J Med, Vol. 370, pp. 1604-1614.

20. *ABT-450/r-ombitasvir and dasabuvir with or without ribavirin for HCV.* **Ferenci, P, et al.** 2014, N Engl J Med, Vol. 370, pp. 1983-1992.

21. *Sofosbuvir and ribavirin in HCV genotypes 2 and 3.* **Zeuzem, S., et al.** 2014, N Engl J Med, Vol. 370, pp. 1993-2001.

22. *All-oral 12-week treatment with daclatasvir plus sofosbuvir in patients with hepatitisC virus genotype 3 infection: ALLY-3 phase III study.* **Nelson, DR, et al.** 2015, Hepatology, Vol. 61, pp. 1127-1135.

23. **Fontaine, H., et al.** *Efficacy of the oral sofosbuvir-based combinations in hcv genotype 4-mono-infected patients from the french observationalcohort anrs co22 hepather.* Vienna, Austria. : 50th Annual Meeting of the European Association for the Study of the Liver, 2015.

24. *Ledipasvir-sofosbuvir with or without ribavirin to treat patients with HCV genotype 1 infection and cirrhosis non-responsive to previous protease-inhibitor therapy: a randomised, double-blind, phase 2 trial (SIRIUS).* **Bourlière, M, et al.** 2015, Lancet Infect Dis, Vol. 15, pp. 397 - 404.

25. *Vaniprevir plus peginterferon alfa-2b and ribavirin in treatment-naive Japanese patients with hepatitis C virus genotype 1 infection: a randomized phase III study.* **Hayashi, N, et al.** 2016, J Gastroenterol, Vol. 51, pp. 390 - 403.

26. *Therapy for hepatitis C--the costs of success.* **Hoofnagle, JH. and Sherker, AH.** 2014, N Engl J Med, Vol. 370, pp. 1552-1553.

27. *Mefenamic acid in combination with ribavirin shows significant effects in reducing chikungunya virus infection in vitro and in vivo.* **Rothan, HA., et al.** 2016, Antiviral Research, Vol. 127, pp. 50-56.

28. *Chikungunya Virus: In Vitro Response to Combination Therapy With Ribavirin and Interferon Alfa 2a.* **Karen, M. Gallegos, et al.** 2016, The Journal of Infectious Diseases, Vol. 214, pp. 1192–7.

29. *Chronic norovirus infection and common variable immunodeficiency.* **Woodward, J., Gkrania-Klotsas, E. and Kumararatne, D.** 2016, Clinical and Experimental Immunology, Vol. 188, pp. 363–370.

30. *Recent advances in the discovery of norovirus therapeutics.* **Kim, Y., et al.** 2015, J Med Chem, Vol. 58, pp. 9438–9450.

31. *Norovirus vaccines and potential antinorovirus drugs: recent advances and future perspectives.* **Kocher, J. and Yuan, L.** 2015, Future Virol, Vol. 10, pp. 899-913.

32. *Interferons and Ribavirin Effectively Inhibit Norwalk Virus Replication in Replicon-Bearing Cells.* **Chang, KO. and George, DW.** 22, 2007, JOURNAL OF VIROLOGY, Vol. 81, pp. 12111-12118.

33. *Chikungunya virus: an update on antiviral development and challenges.* **Kaur, P. and Chu, JJ.** 2013, Drug Discov Today, Vol. 18, pp. 969-983.

34. *A treatment for and vaccine against the deadly Hendra and Nipah viruses.* **Broder, CC, et al.** 2013, Antiviral Res 100:8–13, Vol. 100, pp. 8-13.

35. *Clinical aspects of Marburg hemorrhagic fever.* **Mehedi, M, et al.** 2011, Future Virol, Vol. 6, pp. 1091-1106.

36. *Lassa fever. Effective therapy with ribavirin.* **McCormick, JB, et al.** 1986, N Engl J Med, Vol. 314, pp. 20-26.

37. *Virus taxonomy. Classification and nomenclature of viruses. Ninth report of the International Committee on Taxonomy of Viruses.* **King, AMQ, et al.** San Diego, CA. : Elsevier Academic Press, 2011.

38. *Approved Antiviral Drugs over the Past 50 Years.* **Erik, De Clercq and Guangdi, Lia.** 2016, Clinical Microbiology Reviews, Vol. 29, pp. 695 - 747.

39. *Adherence to combination therapy enhances sustained response in genotype-1–infected patients with chronic hepatitis C.* **McHutchison, J.G., et al.** 6, 2002, Gastroenterology, Vol. 123, pp. 1061 - 1069.

40. *Clustering of membrane receptors can be induced in mature erythrocytes of neonatal but not adult humans. .* **Schekman, R and Singer, S.J.** 1976, Proc.Natl.Acad.Sci.USA,, Vol. 73, pp. 4075-4079.

41. *Method to Enhance the Encapsulation of Biologically Active Molecules in PLGA Nanoparticles.* **Sanju, Sourabhan, Kaladhar, K. and Chandra, P. Sharma.** 3, 2009, Trends Biomater. Artid. Organs, Vol. 22, pp. 211 - 215.

42. *Improved Entrapment Efficiency of Hydrophilic Drug Substance During Nanoprecipitation of Poly(l)lactide Nanoparticles.* **Leena, Peltonen, et al.** 1, 2004, AAPS PharmSciTech , Vol. 5, pp. 1 - 6.

43. *Are high drug loading nanoparticles the next step forward for chemotherapy?* **Joseph, Della Rocca, Demin, Liu and Wenbin, Lin.** 3, 2012, Nanomedicine , Vol. 7, pp. 303- 305.

44. *Preparation, physicochemical characterization and cytotoxicity in vitro of gemcitabine-loaded PEG-PDLLA nanovesicles. .* **Jia, L., et al.** 2010, world journal of gastroenterology, Vol. 16, pp. 1008-1013.

45. *Efficiency of Nanoparticles as a Carrier System for Antiviral Agents in Human Immunodeficiency Virus-Infected Human Monocytes/Macrophages In Vitro, .* **Andreas, R., et al.** 1996, Antimicrobial Agents AndAnd Chemotherapy, pp. 1467–1471.

46. *Boronate functionalized magnetic nanoparticles and off-line hyphenation with capillary electrophoresis for specific extraction and analysis of biomolecules containing cis-diols.* **Dou, P., et al.** 2009, Journal of Chromatography A, Vol. 1216, pp. 7558-7563.

47. *Therapeutic potential of boron-containing compounds.* **Baker, S.J., et al.** 2009, Future Medicinal Chemistry, Vol. 1, pp. 1275-1288.

48. *Novel Functionalized Biodegradable Polymers for Nanoparticle Drug Delivery Systems.* **Kallinteri, P., et al.** 2005, Biomacromolecules, Vol. 6, pp. 1885-1894.

49. *The reaction of phenylboronic acid with nucleosides and mononucleotides.* **Yurkevich, A.M., et al.** 10, 1969, Tetrahedron, Vol. 25, pp. 477- 484.

50. *Measurement of ribavirin and evaluation of its stability in human plasma by high-performance liquid chromatography with UV detection.* **Loregian, A., et al.** 2007, Journal of Chromatography B, Vol. 856, pp. 358-364.

51. *Synthesis and characterization of glycerol-adipic acid hyperbranched polyesters.* **Zhang, T., et al.** 2014, Polymer , Vol. 55, pp. 5065-5072.

52. *Variation in structure and properties of poly(glycerol adipate) via control of chain branching during enzymatic synthesis.* **Taresco, V., et al.** 2016, Polymer , Vol. 89, pp. 41- 49.

53. *Properties of Acyl Modified Poly(Glycerol-Adipate) Comb-Like Polymers and Their Self-Assembly into Nanoparticles.* **Taresco, V, et al.** 2016, Journal of Polymer Science, Part A: Polymer Chemistry, Vol. 54, pp. 3267 - 3278.

54. *Variation in structure and properties of poly(glycerol adipate) via control of chain branching during enzymatic synthesis. .* **Taresco, V., et al.** 2016, Polymer, Vol. 89, pp. 41-49.

55. *Measurement of ribavirin and evaluation of its stability in human plasma by high-performance liquid chromatography with UV detection.* **Loregian, A., et al.** 11, 2007, Journal of Chromatography B, Vol. 856, pp. 358 - 364.

56. **AOAC International.** AOAC Guidelines for Single Laboratory Validation of Chemical methods for dietery supplments and botanicals. [Online] 2002. https://www.aoac.org/aoac_prod_imis/AOAC_Docs/StandardsDevelopment/SLV_Guidelines_Dietary_Supplements.pdf.

57. *EASL Recommendations on Treatment of Hepatitis C 2016.* **European Association for the Study of the liver.** 2016, Journal of Hepatology, pp. 1-42.

58. *Development of a nanoprecipitation method intended for the entrapment of hydrophilic drugs into nanoparticles.* **Bilati, U., Allémann, E. and Doelker, E.** 1, 2005, Eur J Pharm Sci , Vol. 24, pp. 67-75.

59. *Nanoparticles of polyethylene sebacate: a new biodegradable polymer.* **Guhagarkar, SA., Malshe, VC. and Devarajan, PV.** 3, 2009, AAPS PharmSciTech, Vol. 10, pp. 935-942.

60. *Deciphering the mechanism and structural features of polysorbate 80 during adsorption on PLGA nanoparticles by attenuated total reflectance- Fourier transform infrared spectroscopy.* **Abhayraj, S. Joshi, Avinash, Gahane and Ashwani, Kumar Thakur.** 2016, The Royal Society of Chemistry, Vol. 6, pp. 108545–108557.

61. *Friction and adsorption of aqueous polyoxyethylene (Tween) surfactants at hydrophobic surfaces.* **Malgorzata, Graca, et al.** 2, 2007, Journal of Colloid and Interface Science, Vol. 315, pp. 662-670.

62. *Effect of Formulation Compositions on Particle Size and Zeta Potential of Diclofenac Sodium-Loaded Chitosan Nanoparticles.* **Rathapon, Asasutjarit, et al.** 9, 2013, International Journal of Pharmacological and Pharmaceutical Sciences, Vol. 7, pp. 568-570.

63. *Effect of process and formulation variables on the preparation of parenteral paclitaxel-loaded biodegradable polymeric nanoparticles: A co-surfactant study.* **Navneet, Sharma, Parshotam, Madan and Senshang, Lin.** 2016, Asian Journal of Pharmaceutical Science, Vol. 11, pp. 404 - 416.

64. *Modification of the body distribution of poly(methyl methacrylate) nanoparticles in rats by coating with surfactants.* **Tröster, S.D., Müller, U. and Kreuter, J.** 12, 1990, International Journal of Pharmaceutics, Vol. 61, pp. 85 - 100.

65. *Solvent selection in the preparation of poly(DL-lactide) microspheres prepared by the solvent evaporation method.* **Bodmeier, R. and McGinity, J.W.** 1988, International Journal of Pharmaceutics, Vol. 43, pp. 179-186.

66. *Encapsulation of Hydrophilic and Lipophilic Drugs in PLGA Nanoparticles by the Nanoprecipitation Method.* **Barichello, J.M., et al.** 13, 1999, Drug Development and Industrial Pharmacy, Vol. 25, pp. 471 - 476.

67. *Development of Biodegradable Nanoparticles for Liver-Specific Ribavirin Delivery.* **Ishihara, Tsutomu, et al.** 12, 2014, Journal of Pharmaceutical Science, Vol. 103, pp. 4005-4011.

68. *Effect of 5- azacytidine and congeners on DNA methylation and expression of deoxycytidine kinase in the human lymphoid cell lines CCRF/CEM/0 and CCRF/CEM/dCk-1.* **Antonsson, BE., et al.** 1987, Cancer Res 1987, Vol. 47, pp. 3672-3678.

69. *Once daily PSI-7977 plus pegylated IFN/ribavirin in Phase 2B trial: rapid virologic suppression in treatment naive patients with HCV GT2/GT3. .* **Lalezari, J and Lawitz, E & Rodriguez-Torres, M.** S 28, 2011, J Hepatol , Vol. 54.

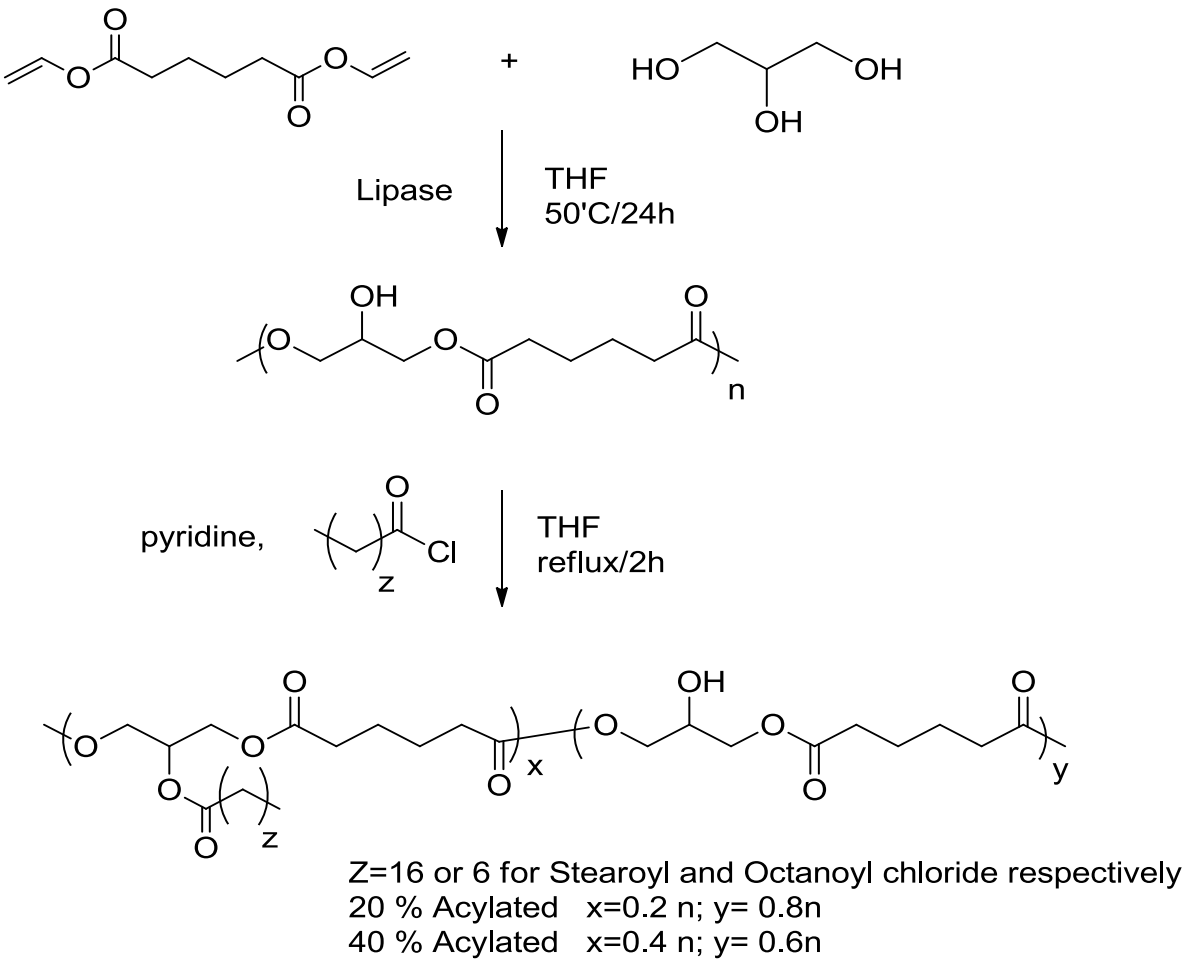

Figure 1: Synthesis of poly(glycerol-adipate), 20% and 40%- C_8 and C_{18} poly(glycerol-adipate)

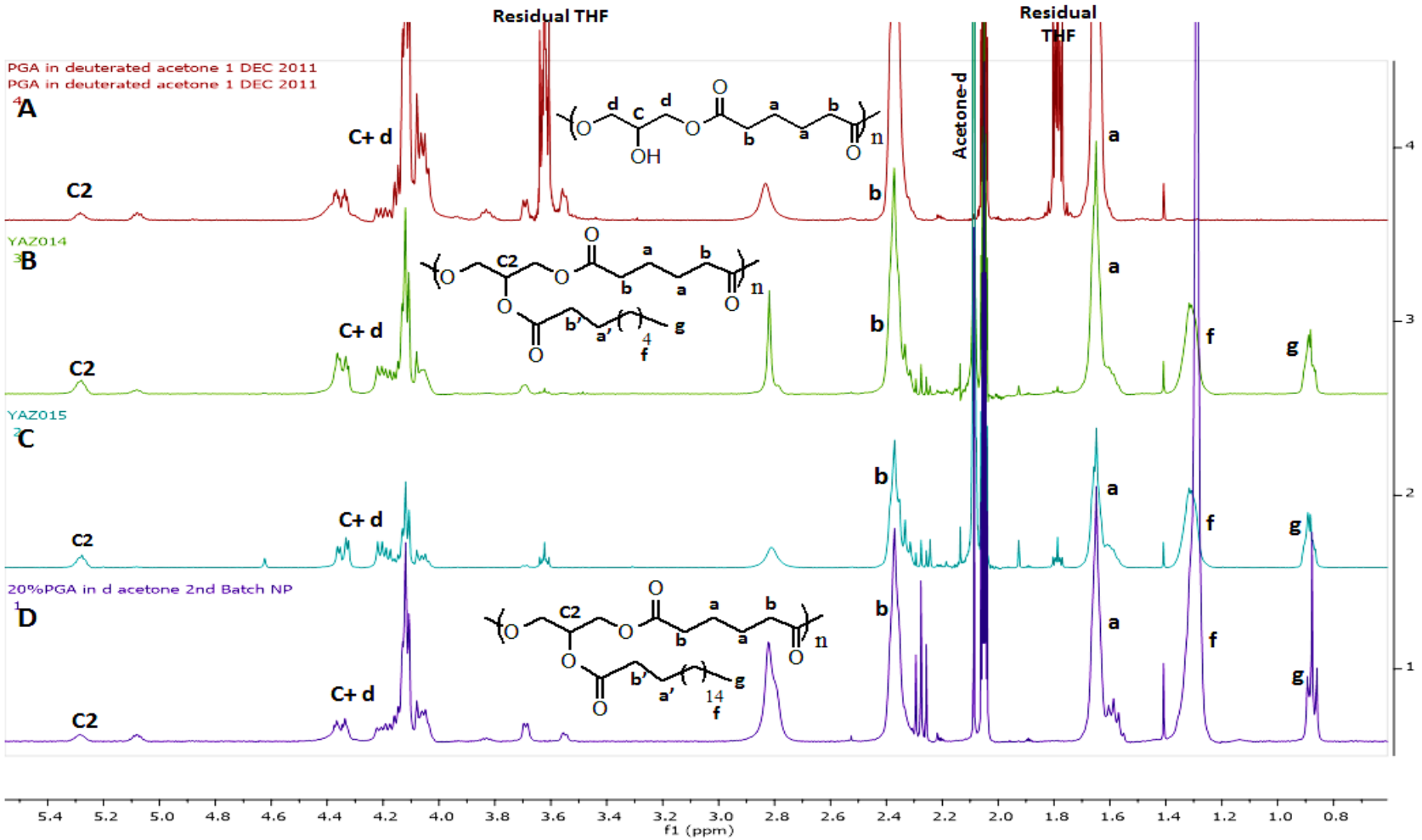

Figure 2: ^{1}H-NMR spectra of (A) PGA, (B) 20%-C_8PGA, (C) 40%-C_8PGA; (D) 20%-C_{18}PGA; acylation of PGA backbone was demonstrated by appearance of methyl (g) and methylene peaks (f) at δ 0.9 or 1.3 ppm.

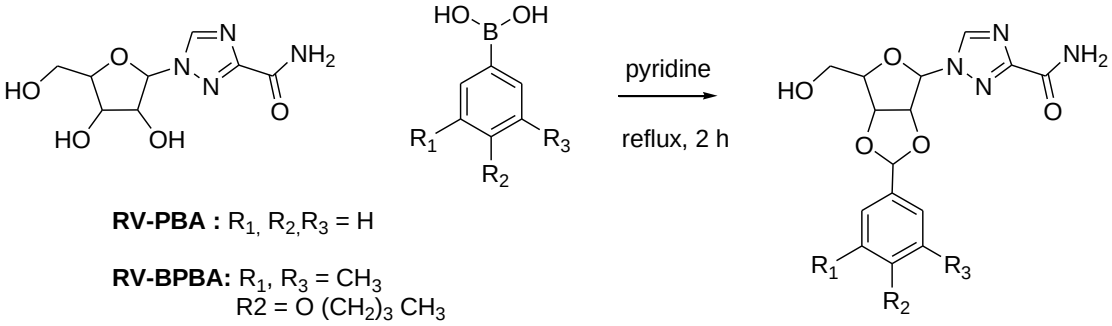

Figure 3: Synthesis of RV-PBA and RV-BPBA.

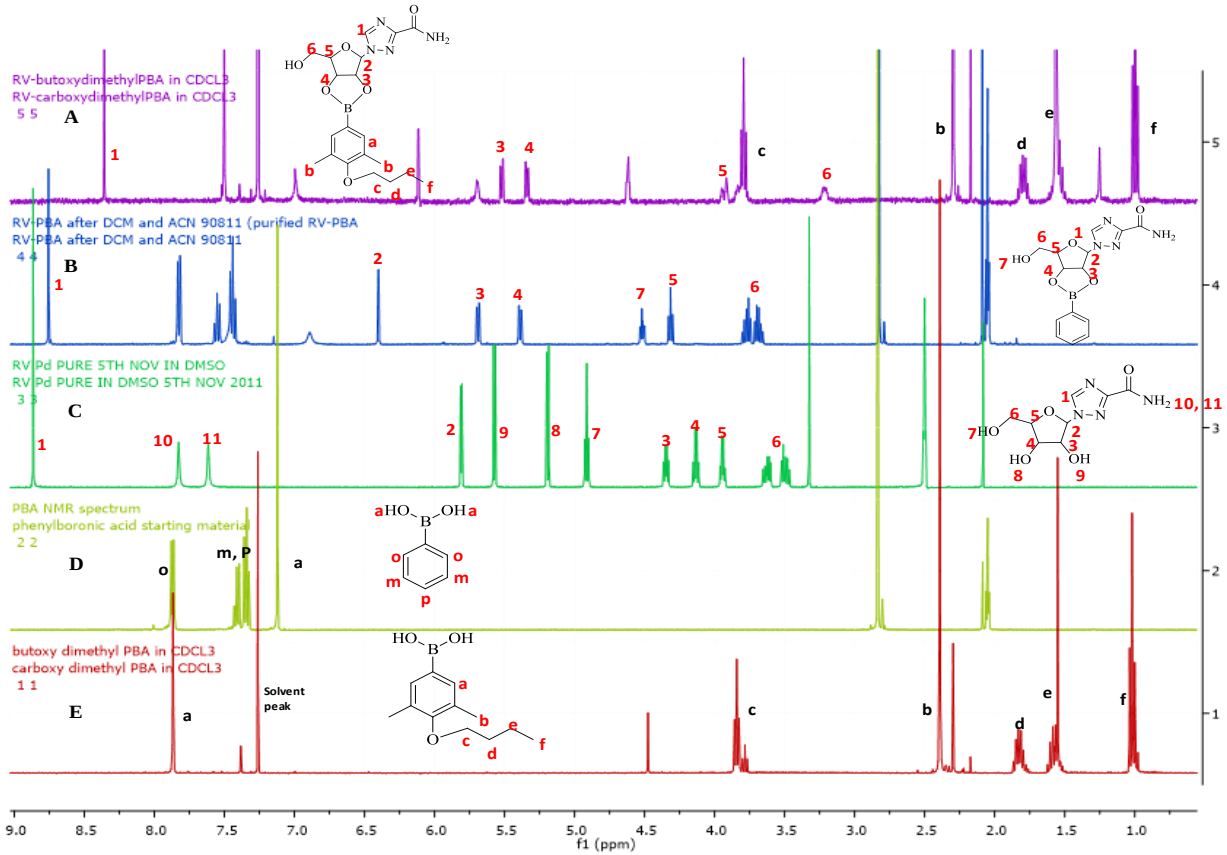

Figure 4: [1]H-NMR spectra of (A) RV-BPBA/ (B) RV-PBA/ (C) RV/ (D) PBA/ (E) BPBA; spectrum demonstrated the formation of RV-BPBA and RV-PBA with around 100% purity as seen from peaks 3' and 4' at δ 5.65 and 5.4 ppm respectively.

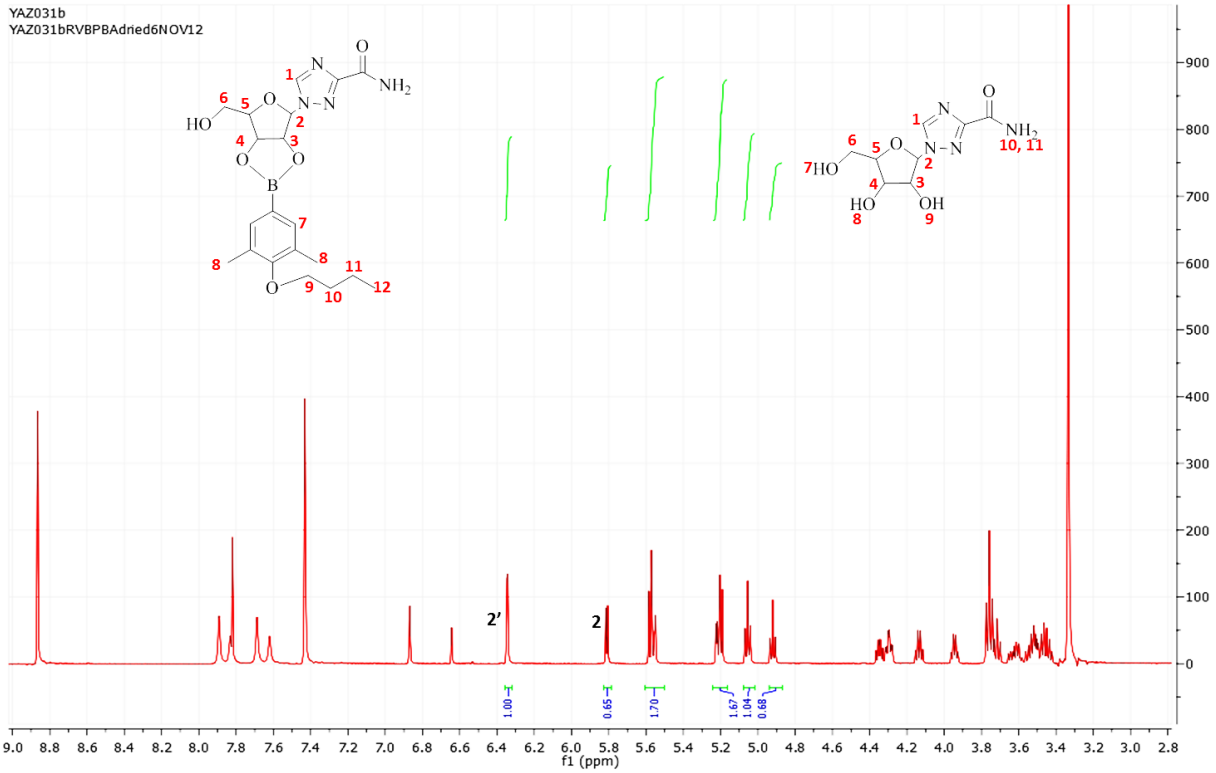

Figure 5: Stability of RV-BPBA in acetone; The degradation of boronic ester was around 39% and it was calculated via dividing peak area of 2 by the summation of peak era of 2'and 2 as follows; the Boronic ester link degradation % = $\left(\frac{\boldsymbol{Integration\ of\ peak\ 2}}{\boldsymbol{sum\ (integration\ of\ peak\ 2 + integraion\ of\ peak2')}}\right) * 100$.

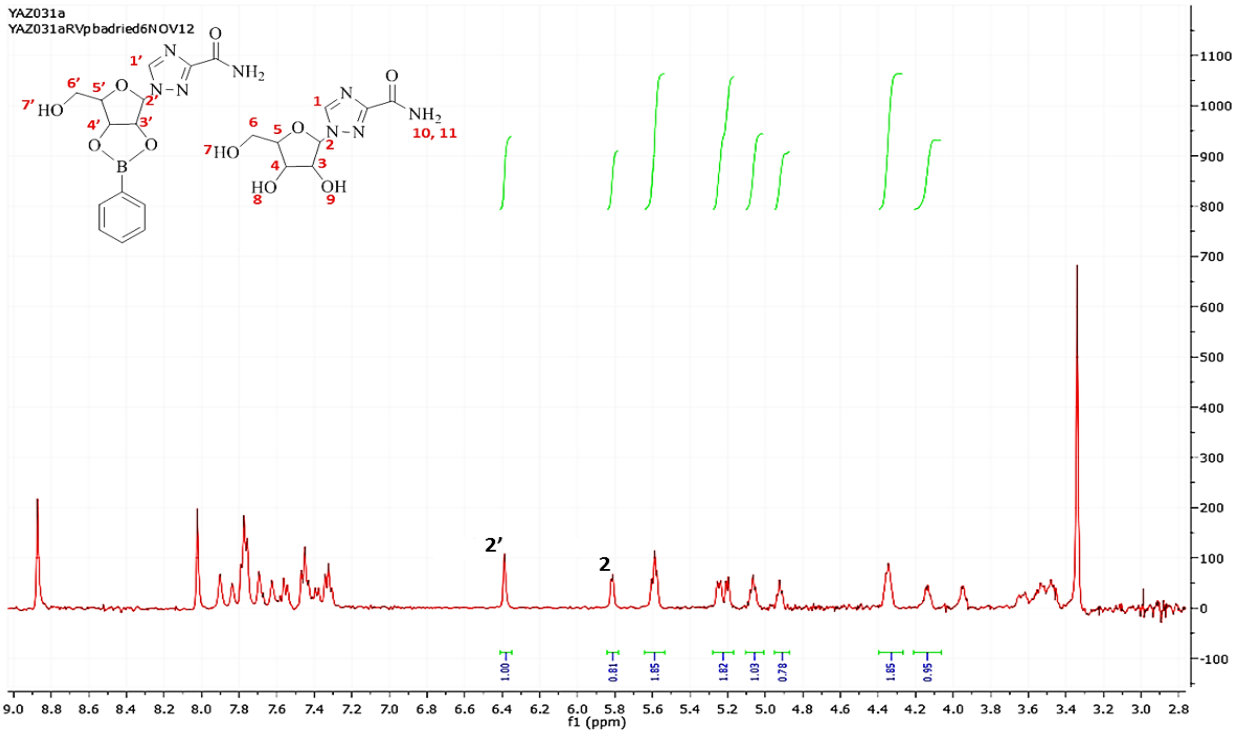

Figure 6: Stability of RV-PBA in acetone; The degradation of boronic ester was around 45% and it was calculated via dividing peak area of (2) by the summation of peak era of 2' and 2 as follows; the Boronic ester link degradation % = $[\frac{\boldsymbol{Integraion\ of\ peak\ 2}}{\boldsymbol{Sum\ (integraion\ of\ peak\ 2 + integraion\ of\ peak\ 2)'}}] * 100$.

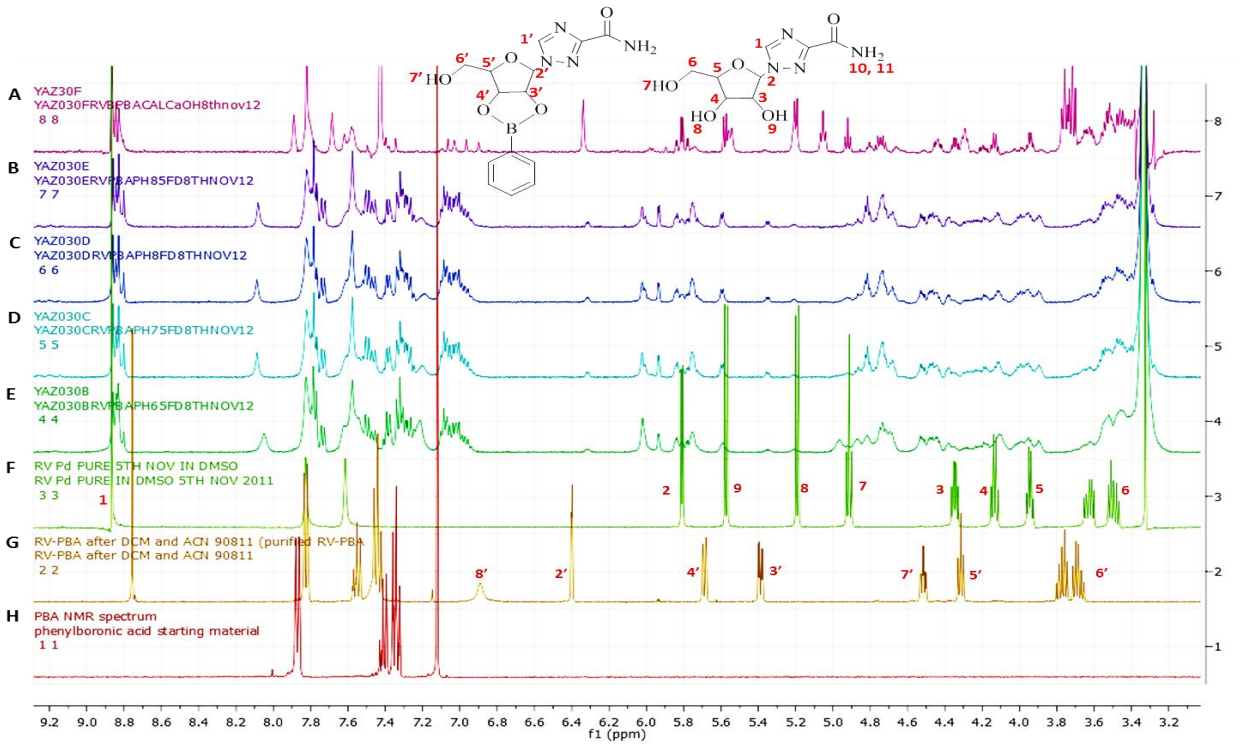

Figure 7: ^{1}H-NMR spectra revealing the stability of boronic ester link of RV-PBA in aqueous media: ^{1}H-NMR spectra of RV-PBA degraded in calcium hydroxide solution 0.3 mM (A) and ammonium phosphate buffer, 250 mM, pH 8.5 (B), pH 8 (C), pH7.5 (D) and pH6.5 (E) in combination of ^{1}H-NMR spectra of pure ribavirin (F), intact RV-PBA (G) and PBA (H), showed that RV-PBA is almost completely degraded in aqueous media and this explains why it was not associated with any improvement of drug loading into NP prepared by different polymers.